Biochemical Pharmacology 79 (2010) 575–586

Contents lists available at ScienceDirect

Biochemical Pharmacology

journal homepage: www.elsevier.com/locate/biochempharm

New caspase-independent but ROS-dependent apoptosis pathways are targeted in melanoma cells by an iron-containing cytosine analogue

Jeannine C. Franke [a,b], Michael Plötz [a], Aram Prokop [c,1], Christoph C. Geilen [a], Hans-Günther Schmalz [d,1], Jürgen Eberle [a,*]

[a] Department of Dermatology and Allergy, Skin Cancer Center Charité, Charitéplatz 1, 10117 Berlin, Germany
[b] Free University of Berlin, Department of Biology, Chemistry and Pharmacy, Takustr. 3, 14195 Berlin, Germany
[c] University of Cologne, Department of Paediatric Oncology, Amsterdamer Str. 59, 50735 Cologne, Germany
[d] University of Cologne, Department of Organic Chemistry, Greinstr. 4, 50939 Cologne, Germany

ARTICLE INFO

Article history:
Received 9 June 2009
Received in revised form 6 September 2009
Accepted 21 September 2009

Keywords:
Melanoma
Apoptosis
Caspase-independent
ROS
Bcl-2
zVAD

ABSTRACT

Chemotherapy resistance and related defects in apoptotic signaling are crucial for the high mortality of melanoma. Effective drugs are lacking, also due to the fact that apoptosis regulation in this tumor is essentially not understood. The cytosine analogue ferropoptoside (N69), which contains an iron carbonyl complex, resulted in strong induction of apoptosis in melanoma cells starting already after 2 h, whereas cytotoxicity remained at a low level. Surprisingly, there was no indication for any caspase activation at early times, although cytochrome *c* was released from mitochondria. Indicative for new proapoptotic pathways was the production of reactive oxygen species (ROS) as an early effect, and the inhibition of apoptosis by the antioxidant vitamin E. Apoptosis was also blocked by exogenous Bcl-2 overexpression and by the pan-protease inhibitor zVAD. However, only zVAD also prevented ROS production, for which Bcl-2 remained without an effect. Thus, new proapoptotic pathways are described here for melanoma cells clearly related to ROS production. A cascade enclosing enhanced levels of intracellular iron, which lead to enhanced ROS production in a Fenton reaction, appears as suggestive. Whereas off-target effects of zVAD appear as upstream, Bcl-2 may exert its inhibitory activity downstream of ROS. New proapoptotic pathways are of particular interest for melanoma as they may open new options for targeting this highly therapy-refractory tumor.

1. Introduction

Incidence of cutaneous melanoma has dramatically increased in last decades in white populations worldwide. Whereas the primary tumor involves the skin, dissemination to visceral organs is incurable, with a median survival time of less than 12 months [1,2]. The high malignancy is based on a pronounced resistance to conventional chemotherapy, related to defects in proapoptotic signaling. Thus, targeting melanoma by efficient induction of apoptosis appears as promising [3,4].

Two main proapoptotic pathways have been described. The extrinsic pathway is initiated by binding of death ligands to cell surface receptors leading to the formation of a death inducing signaling complex, where initiator caspases 8 and 10 are activated [5]. In contrast, the intrinsic apoptosis pathway is triggered by intracellular signals such as cellular and DNA damage, also when caused by chemotherapy. Key events are depolarization of mitochondrial membrane potential, mitochondrial outer membrane permeabilisation (MOMP), release of mitochondrial cytochrome *c* into the cytosol, which results in activation of initiator caspase-9 [3,6,7]. Both pathways may meet at the mitochondria, which are thus of particular importance in apoptosis regulation. Mitochondrial activation is controlled by the family of Bcl-2 proteins, which consists of antiapoptotic proteins (e.g. Bcl-2, Bcl-x_L and Mcl-1), proapoptotic multidomain proteins (Bax and Bak) and proapoptotic BH3-only proteins (e.g. Bad, Puma and Noxa) [8,9]. According to these pathways, caspase cascades appear as central in apoptosis regulation. Initiator caspases cleave and activate downstream effector caspases, which themselves target a number of death substrates to set apoptosis into work [6,10].

Besides caspase-dependent apoptosis, several recent reports are strongly suggestive for alternative, caspase-independent cell death pathways [11]. Thus, cathepsins have been discussed, which may be released from lysosomes into the cytoplasm to contribute to apoptosis [12,13]. Furthermore apoptosis-inducing factor (AIF)

* Corresponding author at: Charité-Universitätsmedizin Berlin, Department of Dermatology and Allergy, Skin Cancer Center Charité (HTCC), Charitéplatz 1, 10117 Berlin, Germany. Tel.: +49 30 8445 4572.
E-mail address: juergen.eberle@charite.de (J. Eberle).
[1] Both authors hold a patent on N69.

0006-2952/$ – see front matter © 2009 Elsevier Inc. All rights reserved.
doi:10.1016/j.bcp.2009.09.022

and endonuclease G, frequently found in the cytosol after induction of apoptosis, may trigger DNA fragmentation in a caspase-independent way [14]. Finally, reactive oxygen species (ROS) have been discussed in relation to apoptosis control. ROS-mediated damage of membrane proteins and polyunsaturated fatty acids may lead to mitochondrial and lysosomal dysfunction [15,16], and ROS-mediated DNA damage may also result in DNA fragmentation and apoptosis [17,18].

New drugs are urgently needed for treatment of metastatic melanoma. In nucleoside analogues, different modifications have been realized in approved drugs, and growing interest also arises in the development of organic metal complexes. Metal compounds offer new mechanisms of drug action, which may not be realized by organic residues [19]. Here, we demonstrate the high proapoptotic potential of a recently described iron-containing cytosine analogue ferropoptoside (N69, 4 g) [20] in human melanoma cells. It appears to target new apoptosis pathways independent of caspase activation but related to the production of ROS.

2. Materials and methods

2.1. Cell culture

Four human melanoma cell lines were investigated: Mel-HO [21], A-375 [22], Mel-2a [23] and SK-Mel-13 [24]. Subclones of Mel-HO and A-375 resulted from stable transfection of a pIRES-Bcl-2 construct (MelHO-Bcl-2, A375-Bcl-2) or the pIRES empty plasmid (MelHO-Mock, A375-Mock), as previously described [25]. The pIRES plasmid originates from Clontech (Palo Alto, CA, USA). Jurkat lymphoma cell line was used as positive control for caspase processing [26]. Melanoma cells were cultured at 37 °C, 5% CO_2 in DMEM (4.5 g/l glucose; Gibco, Invitrogen, Karlsruhe, Germany) supplemented with 10% FCS and antibiotics (Biochrom, Berlin, Germany). Experiments were performed in 6-well plates or 24-well pates (200,000 and 50,000 cells/well, respectively). Treatment with N69 [20] was started after 24 h, whereas control cells received only solvent ethanol.

For growth curves, cell confluence was continuously monitored by real-time cell analysis (RTCA, xCELLigence, Roche diagnostics; Penzberg, Germany). The technique is based on microelectrods integrated in the bottom of each well of special 96-well E-plates. The electric impedence corresponds to the cell density. 10,000 cells were seeded per microtiter well, and treatment started after 24 h. The impedence was determined up to 60 h after seeding with 15 min intervals.

2.2. Quantification of apoptosis and cytotoxicity

For apoptosis quantification, a cell death detection ELISA (Roche Diagnostics, Mannheim, Germany) was used, which detects mono- and oligonucleosomes formed in apoptotic cells. Cytotoxicity was determined in parallel by measuring LDH activity in culture fluids applying a cytotoxicity detection assay (Roche Diagnostics). Protocols were according to the manufacturer with minor modifications [27].

Cell cycle analyses were carried out for detection of hypodiploid nuclei [28]. Cells were harvested by trypsinisation, stained with propidium iodide (Sigma, Taufkirchen, Germany; 200 μg/ml), washed with PBS and analyzed by a FACS Calibur.

For identification of chromatin condensation and nuclear fragmentation in course of apoptosis, cells were harvested by trypsinisation, centrifuged on cytospins and fixed for 30 min in 4% formaldehyde. Cytospins were stained with bisbenzimide (Hoechst-33258; Sigma, Taufkirchen, Germany; 1 μg/ml, 30 min) and examined by fluorescence microscopy. Apoptotic cells were identified by fragmented nuclei or by bright blue-stained nuclei with condensed DNA.

Free 3′-OH DNA termini indicating DNA strand breaks in apoptotic cells were labeled by terminal deoxynucleotidyl transferase (TUNEL) using an in situ cell death detection kit (Roche Diagnostics). Cells were harvested by trypsinisation, centrifuged on cytospins and fixed in 4% paraformaldehyde for 1 h. Cytospins were treated with 0.1% Triton-X-100 in sodium citrate buffer and were incubated with TUNEL reaction mix for 1 h at 37 °C. Apoptotic cells with green nuclei were identified by fluorescence microscopy.

2.3. Mitochondrial membrane potential and lysosomal membrane permeabilisation

For determination of mitochondrial membrane potential, the fluorescent dye JC-1 (5,5′,6,6′-tetrachloro-1,1′,3,3′-tetraethylbenzimidazolocarbocyanine Iodide) was used. Cells were harvested by trypsinisation, stained with JC-1 (Sigma, Taufkirchen, Germany; 2,5 μM, 15 min; 37 °C) and analyzed in PBS buffer (Biochrom, Berlin, Germany) by a FACS Calibur.

For identification of changes in lysosomal pH, cells were stained with acridine orange. It accumulates in lysosomes to give the typical orange staining under the acidic conditions in intact lysosomes (pH 5). After lysosomal membrane permeabilisation, pH increases according to cytoplasmic conditions (pH 7), and the dye changes from orange to green. Following N69 treatment, cells were stained with acridine orange (Sigma, Taufkirchen, Germany; 15 μg/ml, 30 min), harvested by trypsinisation, centrifuged on cytospins and examined by fluorescence microscopy. For time kinetics, cells were harvested by trypsinisation, stained with acridine orange (Sigma, Taufkirchen, Germany; 15 μg/ml, 15 min; 37 °C) and suspended in PBS buffer (Biochrom, Berlin, Germany). Green fluorescence was determined by a FACS Calibur.

2.4. Western blot analysis

For caspase analysis, cells were lysed in CHAPS buffer (Cell Signaling, Frankfurt, Germany). For PARP analysis, cells were lysed in 62.5 mM Tris–HCl, pH 6.8; 6 M urea; 10% glycerol; 2% SDS; 5% β-mercaptoethanol. For Bcl-2 proteins, cells were lysed in 10 mM Tris–HCl, pH 7.5; 150 mM NaCl; 1 mM EDTA; 2 mM PMSF; 1 μM leupeptin; 1 μM pepstatin; 0.5% SDS and 0.5% Nonidet P-40. For cytochrome *c* and AIF analysis, cytosolic and mitochondrial cell fractions were separated by using a mitochondria/cytosol fractionation kit (Alexis, Grünberg, Germany). For cathepsin analysis, cells were lysed with a tissue grinder in 250 mM sucrose, 10 mM Hepes and 1 mM EDTA. Cell lysis was controlled by microscopy. Lysates were centrifuged at 1000 × *g*, and cellular debris were discarded. The supernatant was centrifuged again at 100,000 × *g* for separation of the lysosomal fraction (pellet) and the cytosolic fraction (supernatant).

Protocols for protein extraction and Western blot analysis were described previously [27].

The following primary antibodies were used: caspase-2 (Alexis, rat, 1:200), cleaved caspase-3 (Cell Signaling, rabbit, 1:1000), caspase-6 (Cell Signaling, rabbit, 1:1000), caspase-7 (Cell Signaling, rabbit, 1:1000), caspase-8 (Cell Signaling, mouse, 1:1000), caspase-9 (Cell Signaling, rabbit, 1:1000), PARP (Biomol, mouse, 1:5000), Mcl-1 (Santa Cruz, mouse, 1:200), Bcl-2 (Santa Cruz, mouse, 1:200), Bcl-x_L (Santa Cruz, rabbit, 1:200), Bax (Santa Cruz, rabbit, 1:200), Bak (Dako, rabbit, 1:500), Bad (Cell Signaling, rabbit, 1:1000), Puma (Epitomics, rabbit, 1:1000), Noxa (Pro Sci, rabbit, 1:500), cytochrome *c* (BD Biosciences, mouse, 1:1000), AIF (Santa Cruz, goat, 1:200), anti-Porin 31 HL (VDAC) (Calbiochem, mouse, 1:5000), cathepsine D (Santa Cruz, goat, 1:200), cathepsine L (Santa Cruz, goat, 1:200), β-actin (Sigma, mouse, 1:5000) and

Hsp-60 (Cayman, mouse, 1:200). The following secondary antibodies were used: peroxidase-labeled anti-rabbit, anti-mouse, anti-goat or anti-rat (Dako, Hamburg, Germany; 1:5000).

2.5. Determination of activated caspase-3 and inhibition of caspases and cathepsins

For determination of activated caspase-3, a sandwich ELISA for activated (cleaved) caspase-3 was performed (Cell Signaling, Frankfurt, Germany), which detects endogenous levels of cleaved caspase-3 protein. Mel-HO and A-375 cells were incubated with 20 μM N69 for 6 and 24 h or were treated with 100 ng CH-11 for 24 h as positive control or were left untreated.

Cells were preincubated for 1 h with 10 μM of fluoro-methylketone (fmk)-derivatized oligopeptides, which bind the active sites of caspase-like proteases. The following inhibitors were used: zVAD-fmk (pancaspase/panprotease), zWEHD-fmk (caspase-1), zVDVAD-fmk (caspase-2), zDEVD-fmk (caspase-3), zYVAD-fmk

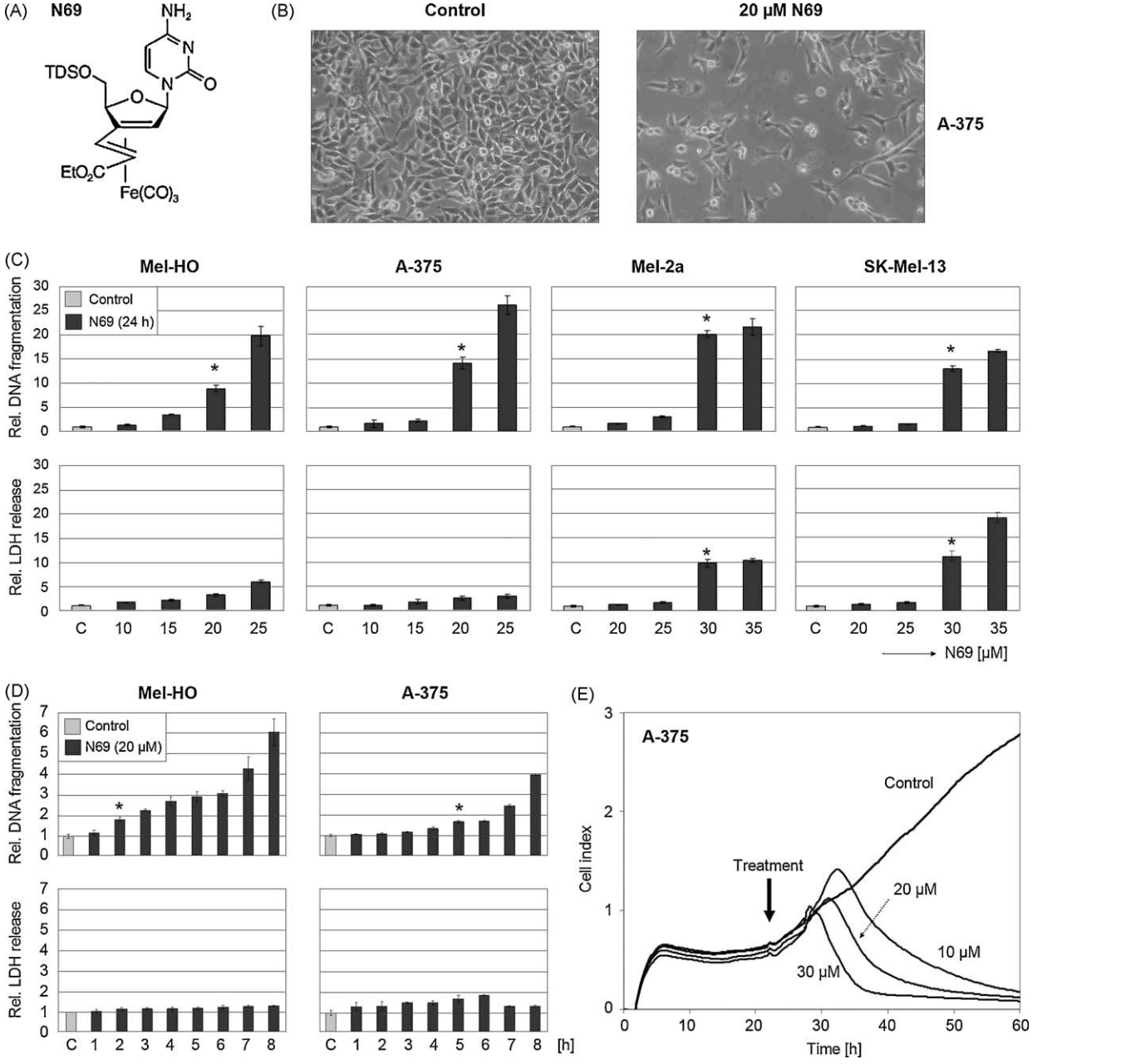

Fig. 1. Dose and time-dependent induction of apoptosis by N69 in melanoma cells. (A) Chemical structure of the iron-containing cytosine analogue N69 (TDS = thexyldimethylsilyl). (B) Example of A-375 cells treated for 24 h with 20 μM N69. Detached and rounded cells are indicative for cell death. (C) Dose-dependent DNA fragmentation indicating apoptosis (upper panel) and LDH-release indicating cytotoxicity (lower panel) are shown for four melanoma cell lines at 24 h after N69 treatment. Concentrations were varied from 10 to 25 μM for highly sensitive cells (Mel-HO, A-375) and from 20 to 35 μM for moderate sensitive cells (Mel-2a, SK-Mel-13). The data of (C and D) represent relative fragmentation values (fold changes versus untreated controls). Values of untreated cells were set to 1. Bars represent mean values ± SD of a representative of three independent experiments, each experiment consisting of triple values. Independent experiments revealed comparable results. (D) Time-dependent DNA fragmentation and LDH-release are shown for Mel-HO and A-375 treated with 20 μM N69. Each time had its own control (not shown), and the values were normalized according the respective controls (C, set to 1). Bars represent mean values ± SD of a representative of two independent experiments, each consisting of triple values. Independent experiments revealed comparable results. (E) Real-time cell analysis (RTCA) is shown for A-375 cells treated with 10, 20 and 30 μM N69. Seeding density was 10,000 cells per microtiter well. Treatment started at 24 h, and monitoring was for 60 h. The determined cell index gives a relative measurement of cell numbers. The experiment was performed three times, each time triple values, which revealed comparable results.

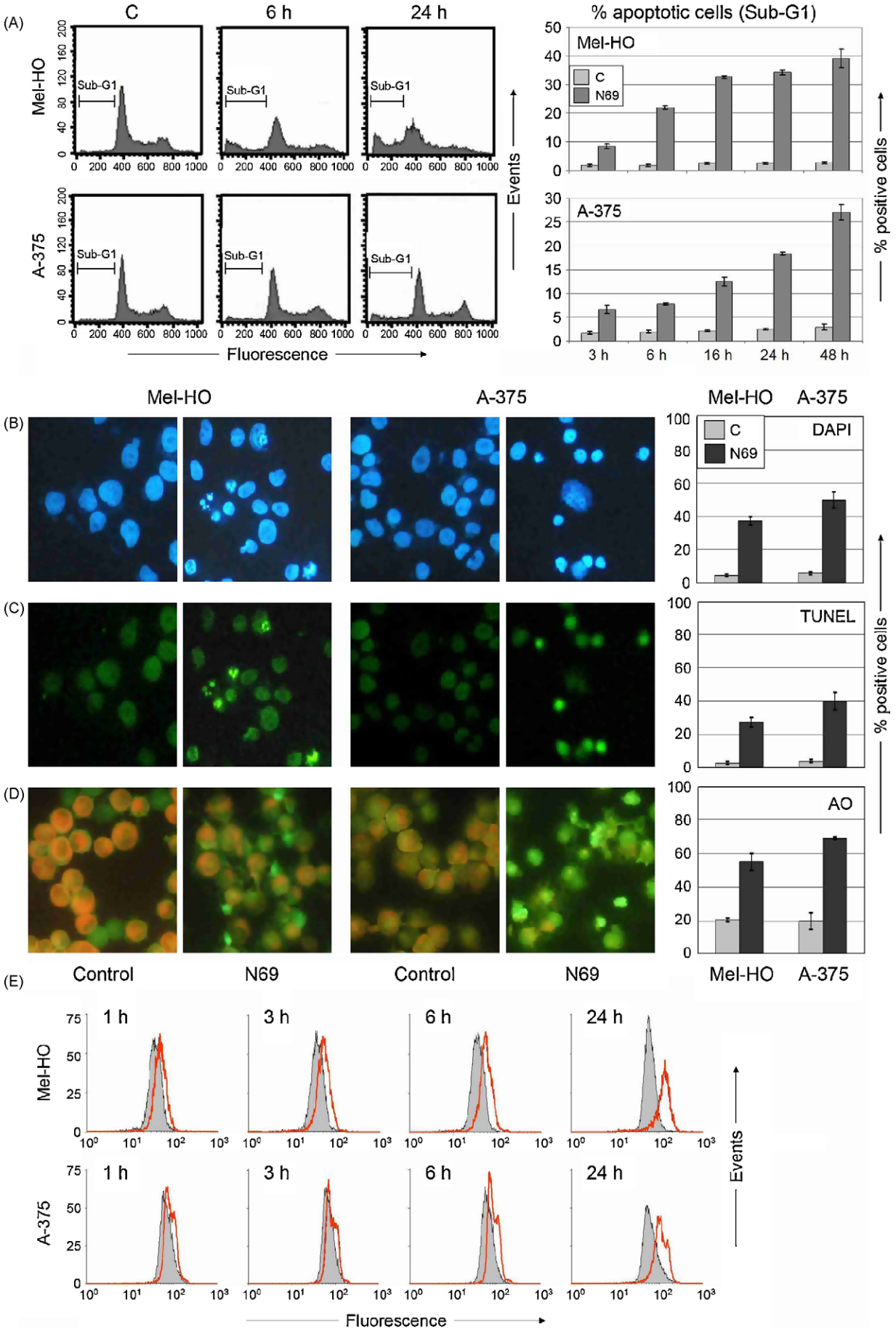
(A)
C
6 h
24 h
Mel-HO
A-375
Sub-G1
Events
Fluorescence
% apoptotic cells (Sub-G1)
Mel-HO
A-375
C
N69
% positive cells
3 h
6 h
16 h
24 h
48 h
(B)
(C)
(D)
DAPI
TUNEL
AO
(E)
Control
N69
1 h
3 h
6 h
24 h

(caspase-4), zVEID-fmk (caspase-6), zIETD-fmk (caspase-8), zLEHD-fmk (caspase-9), zAEVD-fmk (caspase-10) and zLEED-fmk (caspase-13) (R&D Systems, Wiesbaden, Germany).

For inhibition of cathepsins, cells were preincubated for 1 h with different concentrations of fmk-derivatized oligopeptides, which bind the active sites of cathepsine-like proteases. The following inhibitors were used: zFA-FMK (cathepsins B, L), CA-074-Me (cathepsin B) (Calbiochem, Germany).

2.6. Determination of ROS

For measurement of intracellular ROS levels, the fluorescent dye H_2DCFDA (2′,7′-dichlorodihydrofluoresceindiacetate) was used. Cells were stained with H_2DCFDA (Molecular Probes, Invitrogen, Eugene, Oregon, USA; 15 μM, 30 min), harvested by trypsinisation and analyzed in HBSS buffer (Biochrom, Berlin, Germany) by a FACS Calibur.

For ROS scavenging, vitamin E (Fluka, Sigma, Steinheim, Germany) was used in different concentrations, starting from a 50 mM stock solution in ethanol. For positive controls, cells were treated with H_2O_2 (200 μM; 1 h).

3. Results

3.1. Early induction of apoptosis by N69 in melanoma cells

The effects of the iron-containing cytosine analogue N69 (Fig. 1A) on cell death were investigated in four representative human melanoma cell lines (Mel-HO, A-375, Mel-2a and SK-Mel-13). Visible effects as reduced cell numbers, rounded cells and cell detachment were clearly evident after 24 h (Fig. 1B). Induction of apoptosis, as determined after 24 h by DNA fragmentation, was significant at 20 μM (Mel-HO, A-375) and at 30 μM (Mel-2a, SK-Mel-13), respectively. Cytotoxicity, determined by LDH-release, was less pronounced at 20 μM but was also increased after 24 h treatment with 30 μM N69 (Fig. 1C). Investigation of the time dependency of N69-induced apoptosis revealed a significant increase already after 2 h in Mel-HO and after 5 h in A-375. At these early times, cytotoxicity was unaffected, indicating that apoptosis induction was the primary effect (Fig. 1D).

Real-time cell analysis (RTCA) was used to determine the effects on cell confluence. Cell density of N69-treated A-375 cells was continuously monitored for 60 h in microtiterplates. Whereas untreated control cells continuously increased in cell density during this period, N69-treated cells showed a dose-dependent and dramatic decrease of cell density, starting at 6–8 h after N69 was added (Fig. 1E).

Typical hallmarks of apoptosis were seen in N69-treated Mel-HO and A-375 cells, proving the induction of apoptosis. Thus, increased sub-G1 cell populations were evident already at 3 h after N69 treatment and further increased up to 48 h, indicating apoptotic cells with fragmented DNA (Fig. 2A). Chromatin condensation, nuclear fragmentation and nuclear shrinkage were visualized by bisbenzimide staining 48 h after N69 treatment (Fig. 2B), and TUNEL staining indicated an increased number of apoptotic cells with free 3′-OH DNA termini at 48 h (Fig. 2C). Bisbenzimide and TUNEL positivity however appeared as late effects as no significant changes were assessed at 24 h after N69 treatment (data not shown). Quantitative evaluations after 48 h revealed largely concordant results for the three assays, namely 30–50% apoptotic cells upon N69 treatment.

3.2. N69-induced apoptosis in melanoma cells is independent of caspase activation

For exploring the way of N69-induced apoptosis in melanoma cells, involvement of caspases was investigated by Western blot analysis. However, no processing of any of the characteristic proapoptotic caspases (3, 6, 7, 8 or 9) was seen in Mel-HO and A-375 at 6 h or at 24 h after 20 μM N69 treatment. Similarly, no activation of caspase-2 was observed (Fig. 3A). Only after 48 h, typical cleavage products were seen of effector caspase-3 and of the caspase-3 target protein poly(ADP-ribose) polymerase (PARP) (Fig. 3B). Supporting the Western blot data, a highly sensitive sandwich ELISA was performed for the central effector caspase-3, which did not reveal any indication for cleaved caspase-3 at 6 and 24 h after treatment (Fig. 3C).

The results with selective oligopeptide inhibitors for caspases 1, 2, 3, 4, 6, 8, 9, 10 and 13 appeared in parallel, as pretreatment for 1 h (10 μM) remained without effect on the proapoptotic activity of N69 (Fig. 3D). The inhibitory activity of these substances in melanoma cell lines had been demonstrated in a previous study [29]. N69-induced apoptosis was however completely abolished by the pancaspase inhibitor zVAD-fmk (Fig. 3C), which is known to bind a common functional motif of caspases, which is however also shared by other proteases [30].

3.3. Response of mitochondria but no proapoptotic regulation of Bcl-2 proteins

Mitochondrial response in apoptosis is associated with decreased mitochondrial membrane potential. A decreased membrane potential was clearly evident after JC-1 staining and FACS analysis in Mel-HO and A-375 cells already at 1, 3 and at 6 h after treatment with 20 μM N69, again indicating an early apoptotic response (Fig. 4A).

Release of mitochondrial factors into the cytosol and translocation of Bax and Bak are hallmarks in the mitochondrial proapoptotic pathway. For evaluating its contribution in N69-mediated apoptosis, mitochondrial and cytosolic fractions were isolated at 3, 6 and 24 h after treatment with 20 μM N69. Western blot analysis revealed release of cytochrome *c* and apoptosis-inducing factor (AIF) already after 3 h, which further increased with time (Fig. 4B). In parallel, increased levels of Bak but not of Bax were seen in mitochondria (Fig. 4C).

Activation of the mitochondrial pathway was however not linked to an upregulation of the expression levels of proapoptotic multidomain Bcl-2-related proteins (Bax, Bak) or proapoptotic BH3-only proteins (Bad, Noxa, Puma), as determined by Western blot analysis in Mel-HO, A-375, Mel-2a and SK-Mel-13 cells at 24 and 48 h after N69 treatment (20 μM). Rather, upregulation of antiapoptotic Mcl-1 (Mel-HO, Mel-2a, SK-Mel-13) and Bcl-x_L (A-375, Mel-2a, SK-Mel-13) was found in an antiapoptotic response (Fig. 4E).

Fig. 2. Hallmarks of apoptosis after N69 treatment. (A) Increased sub-G1 cell populations were determined by FACS analysis after PI staining for Mel-HO and A-375 treated with 20 μM N69 for 3, 6, 16, 24 and 48 h. (Left side) Examples are shown of control cells, C, cells treated for 6 h and cells treated for 24 h with N69. (Right side) Quantification is shown of all times determined. Means and SDs of triple values in a representative experiment are shown. The whole experiment was repeated once. (B) Chromatin condensation and nuclear fragmentation were visualized by bisbenzimide (DAPI) staining after N69 treatment (20 μM; 48 h). (C) DNA strand breaks were visualized by TUNEL staining after N69 treatment (20 μM; 48 h). (D) Increased acridine orange (AO) staining after N69 treatment (20 μM, 48 h) is visualized by fluorescence microscopy. A change from orange to green reflects an increased lysosomal pH. (A–D) Quantitative evaluations are shown on the right side. Bars represent percentages of positive cells (mean values ± SD of triplicate determinations). All experiments were repeated once, which revealed comparable results. (E) Green fluorescence after acridine orange staining was determined by FACS analysis. Increased levels are shown in Mel-HO and A-375 cells treated for 1, 3, 6 and 24 h with 20 μM N69 (red line, open graphs). Treated cells were compared to non-treated controls (grey). The whole experiment has been repeated once, which revealed comparable results.

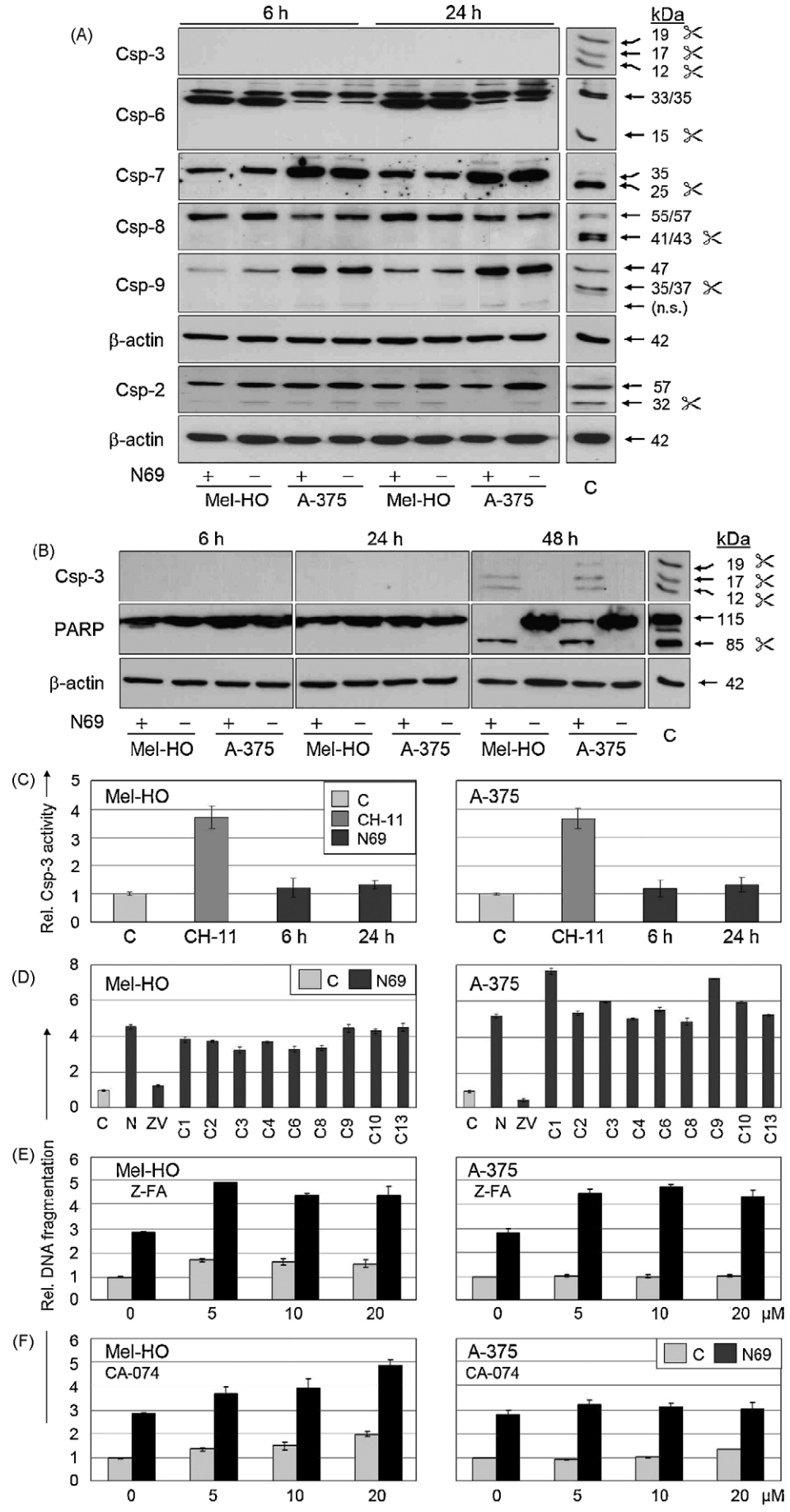
(A)
6 h
24 h
kDa
Csp-3
19
17
12
Csp-6
33/35
15
Csp-7
35
25
Csp-8
55/57
41/43
Csp-9
47
35/37
(n.s.)
β-actin
42
Csp-2
57
32
β-actin
42
N69
+ − + − + − + −
Mel-HO A-375 Mel-HO A-375
C
(B)
6 h
24 h
48 h
kDa
Csp-3
19
17
12
PARP
115
85
β-actin
42
N69
+ − + − + − + − + −
Mel-HO A-375 Mel-HO A-375 Mel-HO A-375
C
(C)
Rel. Csp-3 activity
Mel-HO
C
CH-11
N69
A-375
C CH-11 6 h 24 h
(D)
Mel-HO
C N69
A-375
C N ZV C1 C2 C3 C4 C6 C8 C9 C10 C13
(E)
Rel. DNA fragmentation
Mel-HO
Z-FA
A-375
Z-FA
0 5 10 20 μM
(F)
Mel-HO
CA-074
A-375
CA-074
C N69
0 5 10 20 μM

In addition, we investigated the expression of the transcription factor and apoptosis inducer p53, which has been reported to drive the expression of several proapoptotic Bcl-2 proteins as Bax, Puma and Noxa. Expression of p53 appeared as strongly enhanced in course of N69 treatment in the melanoma cell lines A-375, Mel-2a and SK-Mel-13, but was not regulated in Mel-HO. However, there was no correlation between upregulation of p53 and expression of indicated proapoptotic Bcl-2 proteins (Fig. 4E).

3.4. Involvement of lysosomes

Lysosomal membrane permeabilisation was investigated by staining with acridine orange (AO). Untreated Mel-HO and A-375 cells revealed typical orange staining indicating intact lysosomes, whereas treatment with N69 (20 μM; 48 h) resulted in a characteristic green staining of about 60% of Mel-HO and A-375 cells, indicating lysosomal involvement (Fig. 2D). These changes to green were determined by FACS analysis for Mel-HO and A-375 cells in a time kinetic at 1, 3, 6 and 24 h after treatment with N69. Significant increases in green fluorescence were observed already at 1 h after N69 treatment, which further increased with time, thus proving changes at the lysosomal membranes as associated with early apoptosis effects (Fig. 2E).

Release of lysosomal proteases has been discussed as contributing to apoptosis induction. Also, cathepsin D and L showed some increase in their cytosolic levels after N69 treatment, indicating lysosomal release of cathepsins in course of N69-mediated apoptosis. This release however occurred only lately, after 48 h, likely characterizing the possible involvement of cathepsins as secondary in N69-mediated apoptosis (Fig. 4D). Largely in agreement, the pretreatment of melanoma cells with the cathepsin inhibitors zFA-FMK and CA-074-Me (1 h, 5–20 μM) was not able to prevent N69-induced apoptosis (Fig. 3E and F). The use of higher concentrations of these inhibitors induced apoptosis itself in melanoma cells (data not shown).

3.5. Association of N69-mediated apoptosis and ROS production

Intracellular iron may result in production of ROS. Indeed, significantly increased ROS levels were detected by FACS analysis after H_2DCFDA staining in Mel-HO and A-375 cells at 1, 3 and at 6 h after treatment with 20 μM N69 (Fig. 5A). The role of ROS in N69-induced apoptosis was further investigated by application of the lipophilic antioxidant vitamin E (VitE). Pretreatment for 1 h with VitE was able to block N69-mediated ROS production (Fig. 5B) and also almost completely abolished N69-induced apoptosis (Fig. 5C).

3.6. ROS production is blocked by the panprotease inhibitor zVAD but not by Bcl-2

For better understanding the steps involved in N69-mediated apoptosis in melanoma cells, the effects of characteristic anti-apoptotic agents, namely ectopic overexpression of Bcl-2 and the pancaspase/panprotease inhibitor zVAD were investigated. Subclones of Mel-HO and A-375, stably transfected with a Bcl-2 expression plasmid were completely protected from the proapoptotic effects of N69, as compared to mock-transfected cells (Fig. 6A). Similarly, pretreatment with zVAD was able to completely prevent N69-induced apoptosis in both cell lines (Fig. 3D). However, whereas Bcl-2 overexpression was without an effect on ROS levels indicating its antiapoptotic activity downstream of ROS (Fig. 6B), zVAD also prevented N69-induced ROS production thus indicative for upstream targets (Fig. 6C).

4. Discussion

Induction of apoptosis by intrinsic pathways appears as a critical issue in cancer therapy [4]. For metastatic melanoma however, chemotherapies were not effective so far and are even not able to extend life expectancy of patients [2]. This may be seen as an indication that described intrinsic apoptosis pathways may not be the suitable target in melanoma [31]. Nevertheless, apoptosis is induced in melanoma cells in vitro by strategies such as overexpression of proapoptotic Bcl-2 proteins [31], but these investigations had suggested a predominance of caspase-independent pathways [29,32].

New drugs may have the chance to overcome melanoma therapy resistance, when such alternative pathways are targeted. Organometallic nucleoside analogues are new candidates [19], and for the iron-containing nucleoside analogue ferropoptoside (N69), proapoptotic activity has previously been demonstrated in a lymphoma cell line [20]. Here, we show strong and early induction of apoptosis by N69 in melanoma cells, as proven by independent apoptosis assays which are largely in agreement with recent recommendations for the classification of cell death [33]. In contrast, cytotoxicity appeared as a secondary effect.

However, N69-mediated apoptosis in melanoma cells appeared as distinct from previously described signal transduction pathways. Caspases were clearly not involved in the initial phase and were activated only lately due to cellular amplification loops. In contrast, production of ROS appeared as an early effect, and ROS scavenging by the lipophilic antioxidant vitamin E completely abolished N69-mediated apoptosis. The antioxidative activity of vitamin E had previously been demonstrated in other cellular models [34,35].

ROS are involved in the regulation of different signal transduction pathways including MAP kinases and transcription factors [15], and ROS have also been discussed as contributing to the regulation of apoptosis [36–38]. The mitochondrial respiratory chain is the major source of intracellular ROS, which results in generation of the superoxide anion as the predominant precursor, and in subsequent H_2O_2 production by superoxide dismutase [37]. When interacting with H_2O_2, intracellular iron may trigger the generation of the highly reactive hydroxyl radical in a Fenton

Fig. 3. No early caspase activation by N69. (A) Proteins were extracted from Mel-HO and A-375 cells after treatment with N69 (20 μM, 6 and 24 h, as indicated). Described cleavage products of caspases, indicated by a ✂, were seen only in the positive control (C = doxorubicin-treated Jurkat cells). The illustrated Western blots of N69-treated cells correspond to long-term exposures to X-ray films. Molecular weights are indicated in kDa. N.s. indicates a non-specified band seen in melanoma cells with the caspase-6 antibody. (B) Caspase-3 and PARP cleavage monitored at 6, 24 and 48 h after N69 treatment demonstrate only late activation (48 h). Analysis for β-actin (A and B) demonstrates equal protein loading (50 μg/lane). Experiments were repeated twice, which revealed comparable results. (C) Activated Caspase-3 was determined by ELISA. Mel-HO and A-375 cells were incubated with 20 μM N69 for 6 and 24 h and were compared to non-treated controls kept for the same time (C), set to 1. As positive controls, cells were treated with 100 ng CH-11 agonistic CD95 antibody for 24 h (CH-11). The determinations have been performed 4-times (two independent experiment). Means and SDs of all four values are shown. (D) Relative DNA-fragmentation values (apoptosis) are shown of Mel-HO and A-375 cells treated for 24 h with 20 μM N69 alone (N) as compared to untreated control cells (C). Parallel cultures were preincubated for 1 h before N69 treatment with the pancaspase inhibitor zVAD-fmk (ZV) or with 10 μM of selective peptide inhibitors for caspases 1, 2, 3, 4, 6, 8, 9, 10 and 13 (C1–C13). For each inhibitor, an individual control without N69 was determined, and each value was normalized according to its own control, which had been set to 1 (not shown). Bars represent mean values ± SD of one representative of two independent experiments. Both experiments consisted of triple values and revealed comparable results. (E and F) Relative DNA-fragmentation values (apoptosis), as determined by ELISA, are shown for Mel-HO and A-375 cells pretreated for 1 h with increasing concentrations (0, 5, 10, and 20 μM) of cathepsin inhibitors z-FA (E) and CA-074 (F). Cells were treated for 24 h with 20 μM of N69 (dark bars), and apoptosis was compared to control cultures without N69 (C, light grey). Values were normalized to completely untreated cells, set to 1. Bars represent mean values ± SD of a representative of two independent experiments. Both experiments consisted of triple values and revealed comparable results.

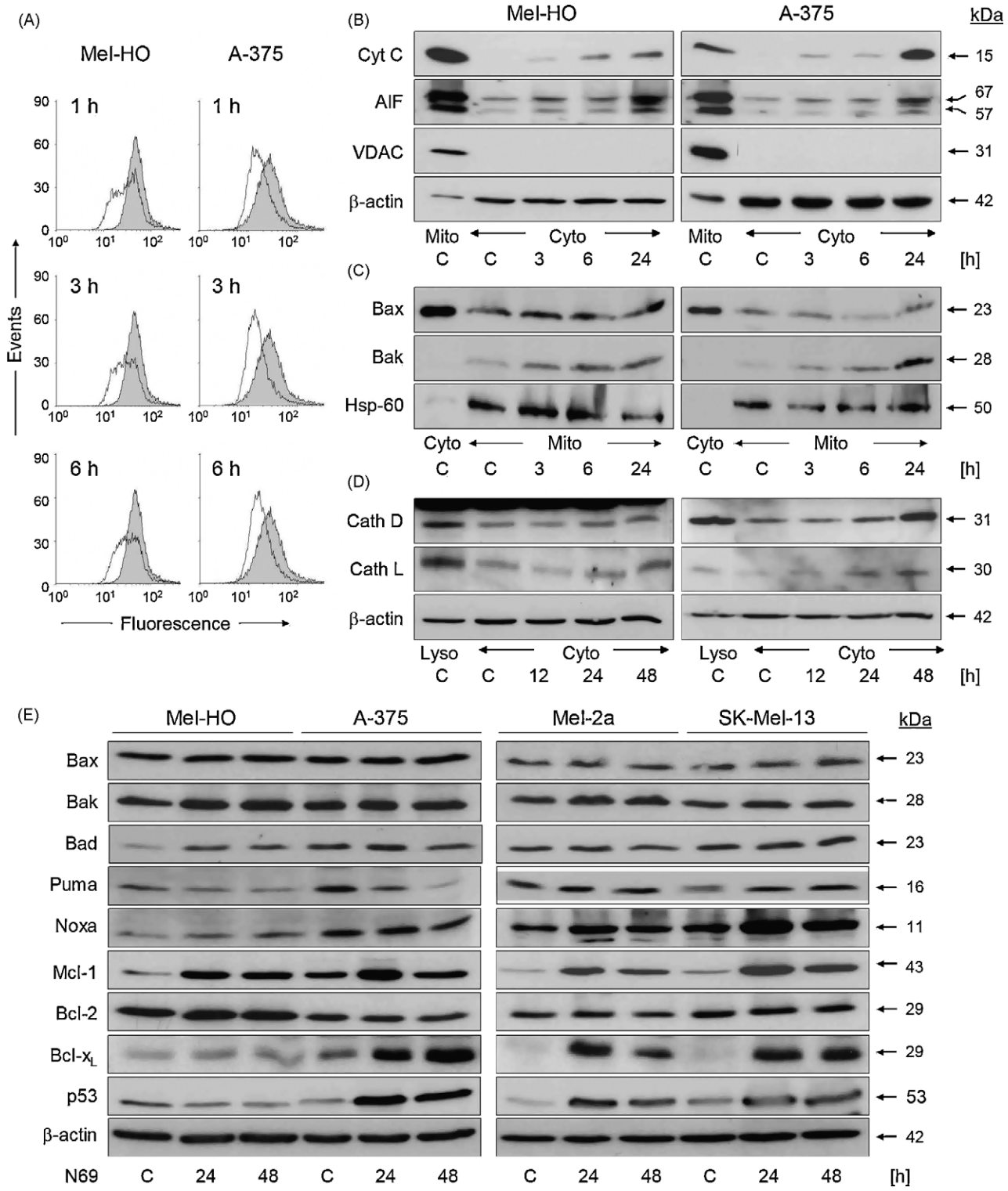

Fig. 4. Response of mitochondria and Bcl-2 proteins. (A) Decreased mitochondrial membrane potential, as determined by FACS analysis after JC-1 staining, is shown for Mel-HO and A-375 treated for 1, 3 and 6 h with 20 μM N69 (open graph) as compared to non-treated controls (grey). The whole experiment has been repeated once, which revealed comparable results. (B) Mitochondrial fractions (Mito) and cytosolic fractions (Cyto) were isolated of Mel-HO and A-375 cells treated with 20 μM N69 for 3, 6 and 24 h. Cytosolic extracts were analyzed by Western blotting for the release of cytochrome *c* and AIF. Treated cells were compared to untreated controls kept for 24 h in parallel (C). Mitochondrial extracts were loaded as additional controls, and analysis of the mitochondrial protein VDAC ruled out any contamination of cytosolic extracts with mitochondria. Beta-actin served as the cytosolic loading control (20 μg/lane). (C) Mitochondrial extracts of N69-treated Mel-HO and A-375 cells were analyzed for translocation of Bax or Bak. Untreated cells were kept in parallel for 24 h (C). Heat shock protein 60 (Hsp-60) showed equal loading of mitochondrial extracts (20 μg/lane). Experiments (B/C) were repeated once, which revealed comparable results. (D) Cytosolic extracts of Mel-HO and A-375 treated with N69 (20 μM; 12, 24 and 48 h) were analyzed for release of cathepsin D and L. Untreated controls were kept for 48 h in parallel (C). Lysosomal extracts were loaded as positive controls. Beta-actin served as the cytosolic loading control (50 μg/lane). The experiment was repeated twice, which revealed comparable results. (E) Antiapoptotic Bcl-2 proteins (Mcl-1, Bcl-2, Bcl-x_L), proapoptotic multidomain Bcl-2 proteins (Bax, Bak), propoptotic BH3-only Bcl-2 proteins (Bad, Puma, Noxa) and p53 were investigated by Western blot analysis. Their expression was determined in four melanoma cell lines treated for 24 and 48 h with 20 μM N69 and compared to untreated controls (C). Beta-actin served as loading control (50 μg/lane). Experiments were repeated once, which revealed comparable results.

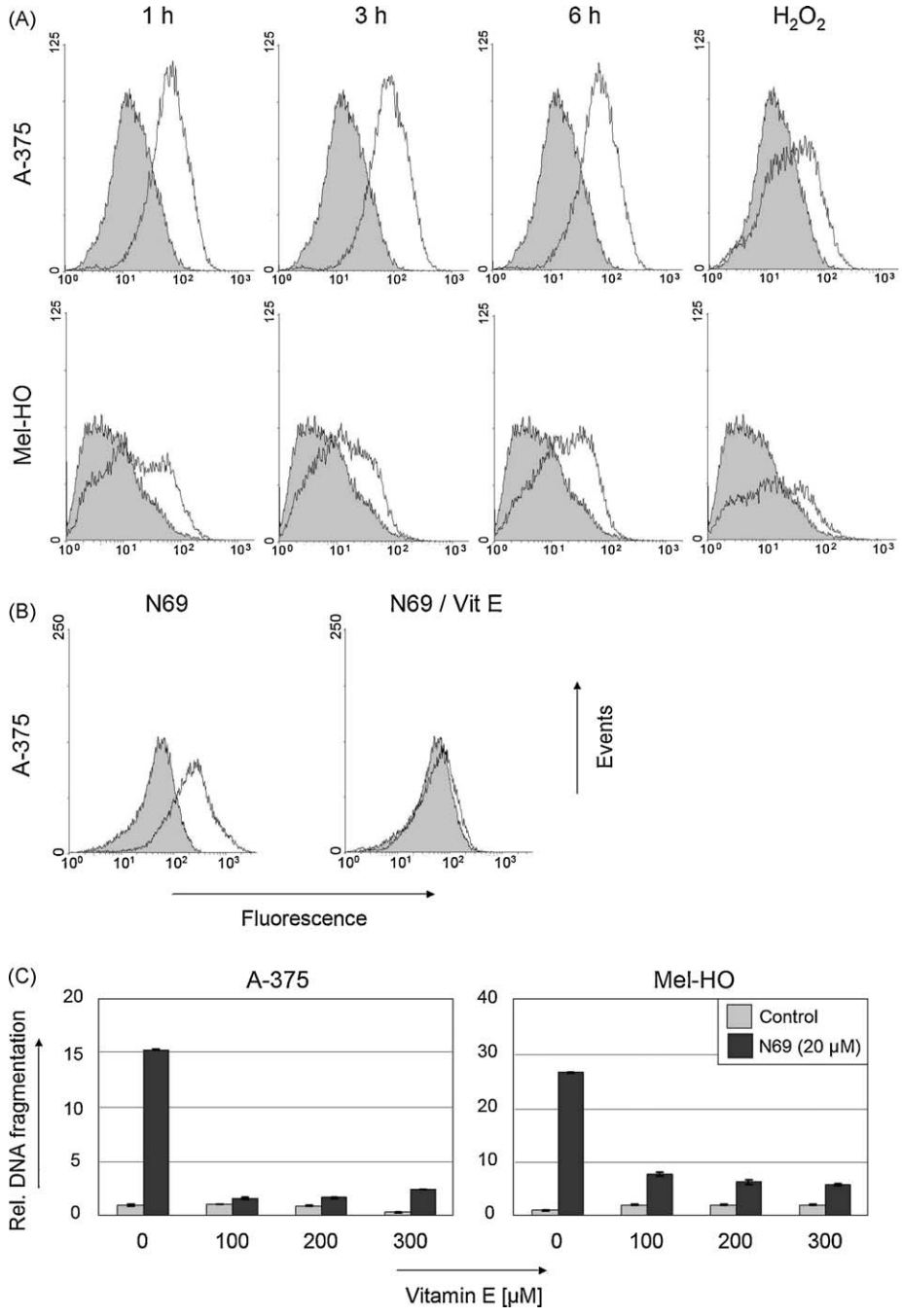

Fig. 5. Involvement of ROS in N69-mediated apoptosis. (A) ROS levels were determined by H_2DCFDA staining and FACS analysis in Mel-HO and A-375 cells at 1, 3 and 6 h after N69 treatment (open graphs) and were compared to untreated controls (grey). H_2O_2-treated cells (200 mM; 1 h) served as positive controls. A shift to higher fluorescence corresponds to increased ROS levels. Experiments were repeated twice, which revealed comparable results. (B) A-375 cells were pretreated for 1 h with 200 μM vitamin E (VitE) before N69 was given (20 μM; 24 h). N69-treated cells (open graphs) were compared to cells without N69 (grey). Experiments were repeated twice, which revealed comparable results. (C) Apoptosis rates are shown for A-375 and Mel-HO cells pretreated for 1 h with increasing concentrations (100–300 μM) of vitamin E (VitE) before N69 treatment (20 μM; 24 h). Comparison was perfomed to non-pretreated cells (0 μM VitE; 20 μM N69, 24 h). Relative DNA-fragmentation rates are shown with respect to untreated controls. Bars represent mean values ± SD of a representative of two independent experiments, each consisting of triple values. Independent experiments revealed comparable results.

reaction [39,40]. Thus, N69-mediated ROS production may result from its capacity as an iron donor, and the nucleoside structure may exert a carrier function.

Different mechanisms have been suggested how ROS may lead to apoptosis and DNA fragmentation, These are again mainly based on caspase activation [37]. Production of ROS has clearly been related to DNA damage, particularly described in skin cells after UV-irradiation. ROS causes different kinds of DNA damage as purine and pyrimidine modification, DNA protein crosslinks, backbone damage and strand breaks [17,18]. One might then expect a classical DNA damage response involving p53 activation, enhanced expression of proapoptotic Bcl-2 proteins and downstream mitochondrial and caspase-9/caspase-3 activation [6]. Cytochrome *c* mobilization and thus its release are also facilitated through ROS-mediated oxidative modification of cardiolipin. Cytochrome *c* is linked to the inner mitochondrial membrane through cardiolipin, and mitochondrial membrane proteins and lipids are primary targets of ROS [15,37].

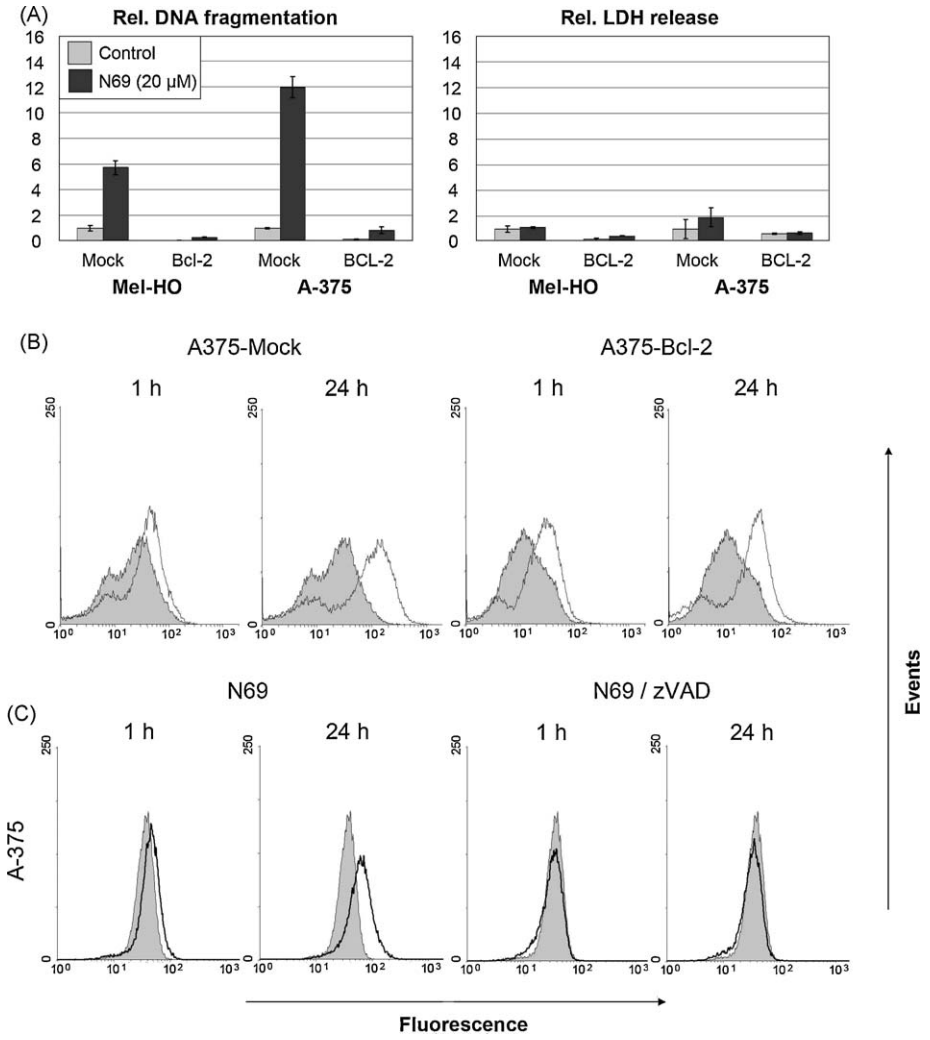

Fig. 6. Effects of Bcl-2 and zVAD on ROS production. (A) Cell clones of Mel-HO and A-375 stably transfected with a Bcl-2-pIRES expression construct (Bcl-2) and pIRES-transfected control clones (Mock) were treated with N69 (20 μM; 24 h). Relative apoptosis and cytotoxicity values were calculated with respect to untreated Mock cells (set to 1). Bars represent mean values ± SD of a representative of three independent experiments, each consisting of triple values. Independent experiments revealed comparable results. (B) ROS levels were determined in a cell clone of A-375 stably transfected with a Bcl-2-pIRES expression construct (Bcl-2) and in a pIRES-transfected control clone (Mock). Cells were treated with N69 (20 μM; 1 and 24 h; open graphs) and compared to untreated controls (grey). The experiment was repeated twice, which revealed comparable results. (C) ROS levels were determined in A375 cells after N69 treatment (20 μM; 1 and 24 h; open graphs) and compared to untreated controls (grey). In addition, cells received pretreatment with zVAD (10 μM; 1 h, right side). Cultures without zVAD are shown on the left side. The experiment was repeated twice, which revealed comparable results.

In agreement with a DNA damage response, we found enhanced p53 levels in three of the melanoma cell lines. Also, mitochondria were activated early in N69-induced apoptosis in melanoma cells, as shown by decreased membrane potential, release of cytochrome *c* and enhanced Bak levels in mitochondria. Bak is considered as mitochondrial protein, which deeper integrates into the mitochondrial membrane upon induction of apoptosis. The higher levels that we observed in mitochondria may indicate that the used extraction protocol distinguishes between strong and lose association. Enhanced Bak levels in mitochondria were also seen in glioblastoma cells after treatment with a NO donor [41] and in hepatoma cells treated with the natural flavonoid luteolin [42].

Thus parts of a DNA damage response appear as activated in melanoma cells by N69. However, apoptosis control in melanoma often looks different. Thus, the role of p53 in melanoma is not clear, and the p53 pathway is believed to be blocked despite the lack of inactivating mutations [31]. In agreement, there was no correlation between p53 upregulation by N69 and the expression of known p53 targets in the Bcl-2 family as Bax, Noxa and Puma [43]. As there was no indication for any downstream caspase cascade in case of N69 in melanoma cells, the described effects of N69 at the mitochondria may lead to a dead end as much as the caspases are concerned. The role of p53 in N69-mediated apoptosis may rather be related to regulation of ROS, as also several REDOX genes have been described as p53 targets [43].

ROS-dependent but caspase-independent apoptosis has been reported in several cell models, as in fibroblasts after treatment with cadmium or curcumin [44,45], in cervical cancer cells treated with arsenic trioxide [46] and in squamous cell carcinoma cells treated with cisplatin [47]. The precise pathways however remained elusive and have been partly explained by the mitochondrial release of AIF and endonuclease G. Melanoma cells revealed relatively high cytoplasmic AIF levels already before treatment, which were enhanced by N69. Given its activity to mediate caspase-independent DNA fragmentation [14], AIF may have an additional contribution in N69-mediated apoptosis.

Also lysosomes and lysosomal release of proteases such as cathepsins have been discussed as inductors of apoptosis either upstream or independent of caspases [12]. Significant lysosomal changes were detected after N69 treatment in melanoma cells, which appeared at early times in parallel to apoptosis induction. However, a cathepsin release was seen only at later times, and

cathepsin inhibitors were not able to prevent early N69-induced apoptosis. Cathepsins may thus contribute to the late phase of N69-mediated apoptosis rather than being involved in its early caspase-independent effects.

The apoptosis pathways activated by N69 in melanoma cells were further illuminated by investigation of the antiapoptotic activities of zVAD and Bcl-2. The pancaspase inhibitor zVAD has already been shown to exert several other activities as a general inhibition of cysteine proteases including cathepsins, papain and legumain [30]. A relation between z-VAD and ROS generation has been already suggested for betulinic acid-induced cell death in prostate cancer cells, where z-VAD-fmk reduced ROS generation as well as DNA fragmentation [48]. We had parallel findings in melanoma cells, namely inhibition of N69-mediated ROS production and inhibition of apoptosis by zVAD. The nature of zVAD targets upstream of ROS however remains unclear both for prostate cancer and for melanoma cells.

Antiapoptotic Bcl-2-related proteins suppress the activities of Bax, Bak and BH3-only proteins and thus prevent MOMP and cytochrome *c* release [7]. It was speculated that they may also be enrolled in control of mitochondrial ROS generation [15,46]. In several studies Bcl-2 overexpression was shown to protect from ROS insults, which was related to enhances activities of antioxidant molecules such as superoxide dismutase and glutathione after Bcl-2 overexpression [49,50]. In melanoma cells, ectopic Bcl-2 overexpression efficiently blocked N69-induced apoptosis, however was without effect on the generation of ROS, thus indicating that Bcl-2 exerts its antiapoptotic activities downstream of primary ROS generation.

Also antiapoptotic changes were observed at the level of the Bcl-2 proteins after N69 treatment, as upregulation of Mcl-1 and Bcl-x_L. These proteins were also upregulated in melanoma cells after treatment with the proteasome inhibitor bortezomib [51]. Such counterregulations may diminish the proapoptotic efficacy of drugs, and strategies for targeting antiapoptotic Bcl-2 proteins, such as by BH3 mimetics [31], might be helpful to further enhance also N69-mediated apoptosis.

The existence of new apoptosis pathways in melanoma cells is demonstrated in the present study. A cascade enclosing intracellular iron, which leads to enhanced ROS production in a Fenton reaction, appears as suggestive. Whether these pathways are only targeted by the drug used here, or whether they are of general importance for melanoma and have been overlooked so far, needs further clarification. New targets may arise with the new pathways addressed here. There is the hope that an Achilles' heal of melanoma may be exposed leading to new treatment options for this highly therapy-refractory tumor.

Acknowledgment

The study was supported by research grants from the Charité – Universitätsmedizin Berlin, by a stipendium of the Sonnenfeld-Stiftung Berlin and by the Deutsche Forschungsgemeinschaft (DFG FO 630).

References

[1] Balch CM, Buzaid AC, Soong SJ, Atkins MB, Cascinelli N, Coit DG, et al. Final version of the American Joint Committee on Cancer staging system for cutaneous melanoma. J Clin Oncol 2001;19:3635–48.
[2] Garbe C, Hauschild A, Volkenandt M, Schadendorf D, Stolz W, Reinhold U, et al. Evidence and interdisciplinary consense-based German guidelines: diagnosis and surveillance of melanoma. Melanoma Res 2007;17:393–9.
[3] Soengas MS, Lowe SW. Apoptosis and melanoma chemoresistance. Oncogene 2003;22:3138–51.
[4] Eberle J, Fecker LF, Forschner T, Ulrich C, Rowert-Huber J, Stockfleth E. Apoptosis pathways as promising targets for skin cancer therapy. Br J Dermatol 2007;156:18–24.
[5] Krammer PH, Arnold R, Lavrik IN. Life and death in peripheral T cells. Nat Rev Immunol 2007;7:532–42.
[6] Riedl SJ, Shi Y. Molecular mechanisms of caspase regulation during apoptosis. Nat Rev Mol Cell Biol 2004;5:897–907.
[7] Chipuk JE, Green DR. How do BCL-2 proteins induce mitochondrial outer membrane permeabilization? Trends Cell Biol 2008;18:157–64.
[8] Daniel PT, Schulze-Osthoff K, Belka C, Guner D. Guardians of cell death: the Bcl-2 family proteins. Essays Biochem 2003;39:73–88.
[9] Hossini AM, Eberle J. Apoptosis induction by Bcl-2 proteins independent of the BH3 domain. Biochem Pharmacol 2008.
[10] Los M, Stroh C, Janicke RU, Engels IH, Schulze-Osthoff K. Caspases: more than just killers? Trends Immunol 2001;22:31–4.
[11] Tait SW, Green DR. Caspase-independent cell death: leaving the set without the final cut. Oncogene 2008;27:6452–61.
[12] Chwieralski CE, Welte T, Buhling F. Cathepsin-regulated apoptosis. Apoptosis 2006;11:143–9.
[13] Broker LE, Kruyt FAE, Giaccone G. Cell death independent of caspases: a review. Clin Cancer Res 2005;11:3155–62.
[14] Lorenzo HK, Susin SA. Therapeutic potential of AIF-mediated caspase-independent programmed cell death. Drug Resist Updat 2007;10:235–55.
[15] Fleury C, Mignotte B, Vayssiere JL. Mitochondrial reactive oxygen species in cell death signaling. Biochimie 2002;84:131–41.
[16] Lockshin RA, Zakeri Z. Apoptosis, autophagy, and more. Int J Biochem Cell Biol 2004;36:2405–19.
[17] Dizdaroglu M, Jaruga P, Birincioglu M, Rodriguez H. Free radical-induced damage to DNA: mechanisms and measurement. Free Radic Biol Med 2002;32:1102–15.
[18] Pelicano H, Carney D, Huang P. ROS stress in cancer cells and therapeutic implications. Drug Resist Updat 2004;7:97–110.
[19] Ott I, Gust R. Non platinum metal complexes as anti-cancer drugs. Arch Pharm (Weinheim) 2007;340:117–26.
[20] Schlawe D, Majdalani A, Velcicky J, Hessler E, Wieder T, Prokop A, et al. Iron-containing nucleoside analogues with pronounced apoptosis-inducing activity. Angew Chem Int Ed Engl 2004;43:1731–4.
[21] Holzmann B, Lehmann JM, Zieglerheitbrock HWL, Funke I, Riethmuller G. Glycoprotein P3.58, associated with tumor progression in Malignant-Melanoma, is a novel leukocyte activation antigen. Int J Cancer 1988;41:542–7.
[22] Giard DJ, Aaronson SA, Todaro GJ, Arnstein P, Kersey JH, Dosik H, et al. In-vitro cultivation of human tumors—establishment of cell lines derived from a series of solid tumors. J Nat Cancer Inst 1973;51:1417–23.
[23] Bruggen J, Sorg C, Macher E. Membrane-associated antigens of human Malignant Melanoma-V—serological typing of cell lines using antisera from nonhuman-primates. Cancer Immunol Immunother 1978;5:53–62.
[24] Carey TE, Takahashi T, Resnick LA, Oettgen HF, Old LJ. Cell-surface antigens of human Malignant-Melanoma—mixed hemadsorption assays for humoral immunity to cultured autologous melanoma cells. Proc Natl Acad Sci USA 1976;73:3278–82.
[25] Raisova M, Hossini AM, Eberle J, Riebeling C, Wieder T, Sturm I, et al. The Bax/Bcl-2 ratio determines the susceptibility of human melanoma cells to CD95/Fas-mediated apoptosis. J Invest Dermatol 2001;117:333–40.
[26] Schneider U, Schwenk HU, Bornkamm G. Characterization of Ebv-genome negative null and T-cell lines derived from children with acute lymphoblastic leukemia and leukemic transformed non-hodgkin lymphoma. Int J Cancer 1977;19:621–6.
[27] Eberle J, Fecker LF, Hossini AM, Wieder T, Daniel PT, Orfanos CE, et al. CD95/Fas signaling in human melanoma cells: conditional expression of CD95L/FasL overcomes the intrinsic apoptosis resistance of malignant melanoma and inhibits growth and progression of human melanoma xenotransplants. Oncogene 2003;22:9131–41.
[28] Nicoletti I, Migliorati G, Pagliacci MC, Grignani F, Riccardi C. A rapid and simple method for measuring thymocyte apoptosis by propidium iodide staining and flow-cytometry. J Immunol Methods 1991;139:271–9.
[29] Oppermann M, Geilen CC, Fecker LF, Gillissen B, Daniel PT, Eberle J. Caspase-independent induction of apoptosis in human melanoma cells by the proapoptotic Bcl-2-related protein Nbk/Bik. Oncogene 2005;24:7369–80.
[30] Rozman-Pungercar J, Kopitar-Jerala N, Bogyo M, Turk D, Vasiljeva O, Stefe I, et al. Inhibition of papain-like cysteine proteases and legumain by caspase-specific inhibitors: when reaction mechanism is more important than specificity. Cell Death Differ 2003;10:881–8.
[31] Eberle J, Kurbanov BM, Hossini AM, Trefter U, Fecker LF. Overcoming apoptosis deficiency of melanoma—hope for new therapeutic approaches. Drug Resist Updat 2007;10:218–34.
[32] Hossini AM, Geilen CC, Fecker LF, Daniel PT, Eberle J. A novel Bcl-x splice product, Bcl-x(AK), triggers apoptosis in human melanoma cells without BH3 domain. Oncogene 2006;25:2160–9.
[33] Kroemer G, Galluzzi L, Vandenabeele P, Abrams J, Alnemri ES, Baehrecke EH, et al. Classification of cell death: recommendations of the Nomenclature Committee on Cell Death 2009. Cell Death Differ 2009;16:3–11.
[34] Wu SJ, Ng LT, Lin CC. Effects of vitamin E on the cinnamaldehyde-induced apoptotic mechanism in human PLC/PRF/5 cells. Clin Exp Pharmacol Physiol 2004;31:770–6.
[35] Gopal DVR, Narkar AA, Badrinath Y, Mishra KP, Joshi DS. Protection of Ewing's sarcoma family tumor (ESFT) cell line SK-N-MC from betulinic acid induced apoptosis by alpha-DL-tocopherol. Toxicol Lett 2004;153:201–12.
[36] Hervouet E, Simonnet H, Godinot C. Mitochondria and reactive oxygen species in renal cancer. Biochimie 2007;89:1080–8.

[37] Orrenius S, Gogvadze V, Zhivotovsky B. Mitochondrial oxidative stress: implications for cell death. Annu Rev Pharmacol Toxicol 2007;47:143–83.
[38] Kiessling MK, Klemke CD, Kaminski MM, Galani IE, Krammer PH, Gulow K. Inhibition of constitutively activated nuclear factor-kappaB induces reactive oxygen species- and iron-dependent cell death in cutaneous T-cell lymphoma. Cancer Res 2009;69:2365–74.
[39] Galaris D, Skiada V, Barbouti A. Redox signaling and cancer: the role of "labile" iron. Cancer Lett 2008;266:21–9.
[40] Valko M, Rhodes CJ, Moncol J, Izakovic M, Mazur M. Free radicals, metals and antioxidants in oxidative stress-induced cancer. Chem Biol Interact 2006;160:1–40.
[41] Jin HO, Park IC, An S, Lee HC, Woo SH, Hong YJ, et al. Up-regulation of Bak and Bim via JNK downstream pathway in the response to nitric oxide in human glioblastoma cells. J Cell Physiol 2006;206:477–86.
[42] Lee HJ, Wang CJ, Kuo HC, Chou FP, Jean LF, Tseng TH. Induction apoptosis of luteolin in human hepatoma HepG2 cells involving mitochondria translocation of Bax/Bak and activation of JNK. Toxicol Appl Pharmacol 2005;203:124–31.
[43] Yu J, Zhang L. The transcriptional targets of p53 in apoptosis control. Biochem Biophys Res Commun 2005;331:851–8.
[44] Shih CM, Ko WC, Wu JS, Wei YH, Wang LF, Chang EE, et al. Mediating of caspase-independent apoptosis by cadmium through the mitochondria-ROS pathway in MRC-5 fibroblasts. J Cell Biochem 2004;91:384–97.
[45] Thayyullathil F, Chathoth S, Hago A, Patel M, Galadari S. Rapid reactive oxygen species (ROS) generation induced by curcumin leads to caspase-dependent and -independent apoptosis in L929 cells. Free Radic Biol Med 2008;45:1403–12.
[46] Kang YH, Yi MJ, Kim MJ, Park MT, Bae S, Kang CM, et al. Caspase-independent cell death by arsenic trioxide in human cervical cancer cells: reactive oxygen species-mediated poly(ADP-ribose) polymerise-1 activation signals apoptosis-inducing factor release from mitochondria. Cancer Res 2004;64:8960–7.
[47] Kim JS, Lee JH, Jeong WW, Choi DH, Cha HJ, Kim DH, et al. Reactive oxygen species-dependent EndoG release mediates cisplatin-induced caspase-independent apoptosis in human head and neck squamous carcinoma cells. Int J Cancer 2008;122:672–80.
[48] Ganguly A, Das B, Roy A, Sen N, Dasgupta SB, Mukhopadhayay S, et al. Betulinic acid, a catalytic inhibitor of topoisomerase I, inhibits reactive oxygen species-mediated apoptotic topoisomerase I-DNA cleavable complex formation in prostate cancer cells but does not affect the process of cell death. Cancer Res 2007;67:11848–5.
[49] Voehringer DW, Meyn RE. Redox aspects of Bcl-2 function. Antioxid Redox Signal 2000;2:537–50.
[50] Tripathi P, Hildeman D. Sensitization of T cells to apoptosis—a role for ROS? Apoptosis 2004;9:515–23.
[51] Fernandez Y, Verhaegen M, Miller TP, Rush JL, Steiner P, Opipari Jr AW, et al. Differential regulation of noxa in normal melanocytes and melanoma cells by proteasome inhibition: therapeutic implications. Cancer Res 2005;65:6294–304.